# TGF-β Ligand Interactions in the Response of *Caenorhabditis elegans* to Bacterial Pathogens

Emma Jo Ciccarelli[1,2], Zachary Wing[1], Moshe Bendelstein[1], Ramandeep Kaur Johal[1], Gurjot Singh[1], Ayelet Monas[1], Cathy Savage-Dunn[1,2*]

[1] Department of Biology, Queens College, CUNY, Flushing, NY

[2] PhD Program in Biology, The Graduate Center, CUNY, New York, NY

* Corresponding author

E-mail: cathy.savagedunn@qc.cuny.edu

**Abstract**

The Transforming Growth Factor beta (TGF-β) family consists of numerous secreted peptide growth factors that play significant roles in cell function, tissue patterning, and organismal homeostasis including wound repair and immunity. Typically studied as homodimers, these ligands have the potential to diversify their functions through ligand interactions that are synergistic, cooperative, additive, and/or antagonistic. In the nematode *Caenorhabditis elegans* there are only five TGF-β ligands, providing an opportunity to dissect ligand interactions in a smaller number of combinations than in vertebrates. As in vertebrates, these ligands can be divided into bone morphogenetic protein (BMP) and TGF-β/Activin subfamilies that predominantly signal through discrete signaling pathways. The BMP subfamily ligand DBL-1 has been well studied for its role in the innate immune response in *C. elegans*. Here we show that all five TGF-β ligands play a role in the immune response. We also demonstrate that multiple TGF-β ligands act cooperatively as part of this response. We show that the two BMP-like ligands – DBL-1 and TIG-2 – function independently of each other in the immune response, while TIG-2/BMP and the TGF-β/Activin-like ligand TIG-3 function cooperatively. We also show that in the response to bacterial pathogen, canonical DBL-1/BMP receptor and Smad signal transducers function, while components of the DAF-7 TGF-β/Activin signaling pathway do not play a role in survival. These results demonstrate a novel potential for BMP and TGF-β/Activin subfamily ligands to interact, and may provide a mechanism for distinguishing the developmental and homeostatic functions of these ligands from an acute response such as the innate immune response to bacterial pathogens.

## Introduction

TGF-β signaling is a highly conserved mechanism that plays a significant role in development in organisms ranging from invertebrates to humans (Attisano and Wrana, 1996; Derynck *et al.*, 1998; Massagué *et al.*, 1998; Morita *et al.*, 2002). This signaling family also plays an important role in the post-developmental adult in maintaining homeostasis and repair (Massagué *et al.*, 1998; Blobe *et al.*, 2000; Massagué, 2000; Massagué, 2012), as well as serving as one of the highly conserved signaling mechanisms involved in the immune response (Medzhitov and Janeway, 1998; Hoffman *et al.*, 1999; Kim *et al.*, 2002; Schulenburg *et al.*, 2004; Millet and Ewbank, 2004; Irazoqui *et al.*, 2008; Partridge *et al.*, 2010). The canonical TGF-β family signaling cascade is initiated by binding of a dimerized ligand to a heterotetrametric receptor complex and mediated through activation of the Smad proteins to regulate transcription (Wrana *et al.*, 1994; Massagué *et al.*, 1998). The human genome contains 33 TGF-β ligands, seven type I receptors, and five type II receptors (Massagué *et al.*, 1998; Huminiecki *et al.*, 2009; Wrana, 2013; Aykul and Martinez-Hackert, 2016). Currently active research is focused on the mechanisms that mediate specific or promiscuous interactions between ligands and receptors, and the consequences for Smad signaling. These mechanisms have profound implications for normal development and disease (Silberstein and Daniel, 1987; Akhurst and Derynck, 2001; Li *et al.*, 2006 Massagué *et al.*, 2008; Pohlers *et al.*, 2009; Zamarron and Chen, 20011; Principe *et al.*, 2014). The number of potential interactions, however, increases the difficulty of these analyses. The reduced repertoire of ligands and receptors in invertebrate organisms provides an opportunity to study ligand-receptor functional interactions more completely. Due to the conservation of TGF-β signaling pathways, studies in the genetically tractable organisms Drosophila and *C. elegans* have resulted in insights into signaling in all organisms.

In *C. elegans*, there are five ligands associated with TGF- β signaling: DBL-1, DAF-7, TIG-2, TIG-3, and UNC-129. Both DAF-7 and TIG-3 are most appropriately classified as TGF-β/Activin like ligands whereas DBL-1 and TIG-2 share the most similarity with the BMP ligands in mammals (Harpin, 2004; Patterson and Padgett, 2000). Of the five TGF-β ligands in *C. elegans*, only two have well characterized signaling pathways through which they signal (Patterson and Padgett, 2000; MacNeill *et al.*, 2009). The TGF-β-like ligand DAF-7 is the regulator of the dauer pathway and its expression in favorable conditions prevents entry into the dauer larval stage (Ren *et al.*, 1996; Schackwitz *et al.*, 1996; Inoue and Thomas, 2000). The BMP-like ligand DBL-1 activates the BMP like pathway in the worm and plays a significant role in development (Suzuki *et al.*, 1999; Yoshida *et al.*, 2001; Wang *et al.*, 2002). UNC-129, TIG-2, and TIG-3 have been classified (as BMP-like or TGF-β-like) based on their structural characteristics, but have not been fully associated with all members of either the BMP-like or TGF-β-like signaling pathways in *C. elegans* (Harpin, 2004; Patterson and Padgett, 2000).

Previous work from our lab and others has demonstrated that the BMP homolog DBL-1 functions in the innate immune response of *C. elegans* to pathogenic bacteria and fungi by inducing the expression of antimicrobial peptide genes in response to pathogen exposure. (Ciccarelli *et al.*, 2023; Mallo *et al.*, 2002; Zugasti and Ewbank, 2009; Zhang and Zhang, 2012). Here we demonstrate that the DBL-1 ligand is only one of four TGF-β family ligands with a significant and consistent role in the immune response to two gram-negative bacterial pathogens. We show that in response to either *Serratia marcescens* or *Photorhabdus luminescens*, multiple TGF-β family ligand mutants have a significant reduction in survival compared to control

animals. We also demonstrate that two BMP-like ligands, DBL-1 and TIG-2, act independently of each other. In contrast, we have shown a non-additive relationship between TIG-2/BMP and the TGF-β-like ligand TIG-3, suggesting a cooperative role for these two distinct ligands in the immune response. Finally, we have identified signaling components with similar phenotypes to TIG-2 and TIG-3 in response to bacterial pathogen. Our studies thus uncover novel signaling paradigms that may act more broadly to distinguish distinct physiological outcomes regulated by TGF-β ligands.

## Materials and Methods

### Nematode Strains and Growth Conditions

*C. elegans* were maintained on *E. coli* (DA837) using EZ worm plates containing streptomycin. Worms were maintained at 20 $^{o}$C, except in experiments using dauer pathway mutants. These strains were maintained at 15 $^{o}$C to prevent entry into dauer. The N2 strain is used as a control. All strains used in this study are: N2, *daf-1,(m40) daf-7(m62), daf-8(e1398), daf-14(m77), sma-2(e502), sma-3(wk30), sma-4(jj278), sma-6(wk7), tig-2(ok3336), tig-2(ok3416), tig-3(tm2092), unc-129(ev554), daf-7(m62);dbl-1(wk70), tig-2(ok3416)dbl-1(wk70), tig-2(ok3416); unc-129(ev554), tig-3(tm2092);tig-2(ok3416), tig-3(tm2092); unc-129(ev554), tig-3(tm2092); tig-2(ok3416); unc-129(ev554), pdbl-1::*GFP.

### Bacteria

Control bacteria in all experiments is *E. coli* strain DA837, cultured at 37$^{o}$C. *S. marcescens* strain Db11 cultured at 37$^{o}$C and *P. luminescens* cultured at 30$^{o}$C were used for bacterial pathogen in survival analyses. *S. marcescens* (db11) is seeded on EZ worm plates containing streptomycin

and grown overnight at 37ºC. *P. luminescens* is seeded on EZ worm plates with no antibiotic and grown overnight at 30ºC.

**Survival Analysis**

Survival plates were prepared at least one day prior to use. Each plate was seeded with 500µl pathogenic bacteria in a full lawn. FuDR was used to prevent reproduction, at a concentration of 50 µM per plate. This was done to reduce the incidence of matricide during survival analysis. Survivals were conducted at 20 ºC, except survivals using dauer pathway mutants, which were conducted at 15 ºC to minimize dauer entry (unless where otherwise stated). Survival analyses were repeated for all ligand experiments and DBL-1 pathway experiments. All graphs made using GraphPad Prism and statistical analysis performed using Logrank/Mantel Cox test.

**Fluorescence Imaging**

Fluorescence imaging of the *dbl-1p::*GFP transcriptional reporter strain were done using a Zeiss ApoTome with AxioVision software and a (20X) objective. Exposure times were kept consistent. Image analysis and fluorescence intensity measurements were done using ImageJ software. Fluorescence intensity was measured for 10 nuclei in each of four worms per bacterial exposure condition.

**qRT-PCR Analysis**

qRT-PCR analysis was performed on collected samples of N2 control animals with or without 24-hour *P. luminescens* pathogen exposure. RNA was obtained by a previously described protocol (Yin *et al.*, 2015) and followed by use of the Qiagen RNeasy miniprep kit (Cat. No.

74104). cDNA was made using SuperScript IV VILO Master Mix (Cat. No.11756050) from Invitrogen, Waltham, MA. qRT-PCR analysis was done using Power SYBR Green PCR Master Mix (Cat. No. 4367659) from Applied Biosystems, Waltham, MA. qRT-PCR was repeated on separate biological replicates. Delta delta Ct analysis was done using Applied Biosystems and StepOne software. Graphs made using GraphPad Prism software.

**Structural Modeling**

SignalP 6.0 was used to predict the signal sequences for TIG-2 and TIG-3 Isoform B. No signal sequence for TIG-3 Isoform A could be determined. The prodomain and mature ligand are defined using a consensus cleavage site (Wisotzkey and Newfeld, 2020). Dimers were modeled using the ColabFold (version 1.5.2) implementation of AlphaFold2-multimer (version 3). The AlphaFold2_mmseqs2 notebook was run under the default settings. The AlphaFold model assigned rank 1 was selected for visualization and analysis. Dimeric interactions were analyzed using UCSF ChimeraX (version 1.5) for AlphaFold structures. The ChimeraX "alphafold contacts" command was applied to identify interchain residue contacts and their associated Predicted Aligned Error (PAE) value. A dimer-interface residue is included in the "Interface" sequence track for AlphaFold complexes if it is within a distance of 4 Å to its partner and the positional error for the residue pair is low (PAE < 5 Å). Additionally, the contacts command was used to discover potential interchain disulfide interactions defined as interchain cysteine pairs less than 8 Å apart with a corresponding PAE under 5 Å.

## Results

### The BMP-like Ligands DBL-1 and TIG-2 are Independently Required for *C. elegans* Survival on Bacterial Pathogen

*C. elegans* has five TGF-β like ligands: DBL-1, DAF-7, UNC-129, TIG-2, and TIG-3. It is established that loss of DBL-1 results in reduced survival of animals on bacterial pathogen (Ciccarelli *et al.*, 2023; Mallo, 2002). DBL-1 is one of two BMP-like ligands in *C. elegans*. In a variety of physiological contexts, heterodimers of BMP ligands are functionally required or outperform homodimers (Tillet *et al*., 2018; Little and Mullins, 2009; Kim *et al.*, 2019; Shimmi *et al.*, 2005). We therefore considered the possibility that DBL-1/BMP functions with the other BMP-like ligand in the worm, TIG-2. The DBL-1 pathway has been quite thoroughly studied in the response to exposure to the gram-negative bacterium *Serratia marcescens*, upon which survival of the worm is significantly hindered due to colonization of the gut when the pathogen is supplied in place of the normal bacterial food source (Mallo, 2002). To test the role of TIG-2/BMP, we quantified survival of two *tig-2* mutant strains on *S. marcescens* and compared these survival rates to *dbl-1* and N2 (wild type) control. We used *tig-2(ok3336),* a 500 bp deletion allele and *tig-2(ok3416),* a 800 bp deletion allele and found that both *tig-2* mutant strains resulted in reduced survival against bacterial infection (Fig. 1A). Survival rates for both *tig-2* mutant strains were significantly different compared to control, although the larger deletion allele resulted in a more pronounced survival defect than the 500bp deletion that was similar to the survival rate seen in *dbl-1* mutants. We further tested the effect of mutating *tig-2* on immunity by analyzing the survival of *tig-2* mutant animals on the more virulent *P. luminescens* bacteria. We found that *tig-2* mutants survived significantly more poorly than control animals (Fig. 1B). Interestingly, we found that *tig-2* mutants had an even more pronounced susceptibility to *P.*

*luminescens* infection than *dbl-1* mutants, suggesting a more significant role for TIG-2 in response to *P. luminescens* infection.

Given that both of these BMP ligands function in the *C. elegans* immune response, we next considered whether they act independently or together by determining the phenotype of double mutants. If these ligands act independently, then we expect the double mutant to have a more severe phenotype than the single mutants, reflecting the disruption of two independent pathways. If they act together, such as in a heterodimer, then we expect the double mutant to have the same phenotype as the single mutants due to the failure of individual ligands to provide physiological function. When grown on *P. luminescens*, *tig-2dbl-1* double mutant animals demonstrated a more pronounced reduction in survival compared to either the *tig-2* or *dbl-1* single mutant animals (Fig. 1C). Our survival analysis shows an additive effect of these two mutations combined. These results indicate that the two BMP like ligands – DBL-1 and TIG-2 – act independently of each other in the response to this bacterial pathogen.

At the time of these experiments, no phenotype had been reported for *tig-2* mutants, so we were encouraged to have identified a biological function for this ligand. To rule out a general effect on lifespan, we followed our survival analysis with a lifespan on control *E. coli* bacteria. Both *tig-2* mutants displayed a lifespan similar to control animals (Fig. S1). Animals mutant for *dbl-1* also had an unaffected lifespan on control bacteria, as expected. These results indicate that the reduced survival of *tig-2* on bacterial pathogen is specific to its susceptibility to infection, and not reflective of a lifespan phenotype. Together these results demonstrate significant roles for the

two BMP-like ligands – DBL-1 and TIG-2 – in the response to pathogenic bacterial infection, although independent of each other.

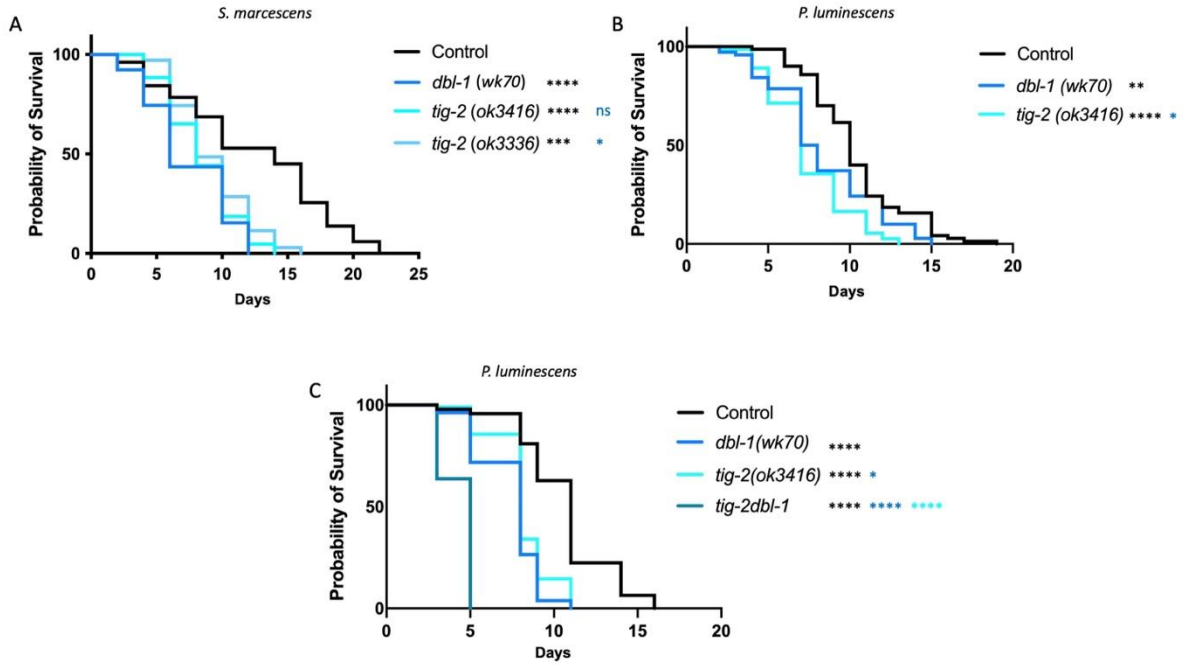


**Figure 1. The BMP-like Ligands DBL-1 and TIG-2 are Required for *C. elegans* Survival on Bacterial Pathogen**.

**A**. Survival analysis of *dbl-1(wk70)* and two *tig-2* mutants (*tig-2(ok3416)* and *(tig-2(ok3336)*) on *S. marcescens* bacteria. N values: Control (51), *dbl-1* (39), *tig-2* (43), *tig*-2 (35). **B.** Survival analysis of *dbl-1(wk70)* and *tig-2(ok3416)* on *P. luminescens* bacteria. n values: Control (70), *dbl-1* (70), *tig-2* (73). **C.** Survival analysis of *tig-2dbl-1* double mutant on *P. luminescens.* n values: Control (94), *dbl-1* (53), *tig-2* (97), *tig-2dbl-1* (55). Statistical analysis done using Log-rank (Mantel-Cox) Test. ns $p > 0.05$; * $p \leq 0.05$; ** $p \leq 0.01$; **** $p < 0.0001$. Black asterisks denote significance relative to control, blue is significance relative to *dbl-1*, and teal is significance relative to *tig-2*.

**Five TGF-β Ligands Demonstrate Involvement in Survival Against Bacterial Infection**

We next were interested in determining if the remaining TGF-β ligands – DAF-7, UNC-129, and TIG-3 – play a role in the *C. elegans* immune response. DAF-7 is well characterized as the ligand in the dauer pathway and *daf-7* mutants demonstrate a high incidence of dauer when grown at 20 $^{o}$C. For this reason, the strains analyzed alongside *daf-7* were all grown to the fourth larval stage (L4) at 15$^{o}$C and shifted to 20 $^{o}$C when moved to pathogen plates. UNC-129 and TIG-3 are "orphan" ligands, without complete TGF-β signaling pathways associated with the ligands.

We found that in mutants of any of the five TGF-β ligands, survival against pathogenic *P. luminescens* infection is significantly reduced, with variability between trials for some ligands (Fig. 2A and Fig. 2B). In particular, *unc-129* mutants have variable survival outcomes. Surprisingly, *dbl-1* mutant animals also have a variable survival pattern on *P. luminescens*, in spite of their well characterized susceptibility to a variety of bacterial and fungal pathogens. In contrast, TIG-2, TIG-3, and DAF-7 show consistently significant susceptibility in response to *P. luminescens*, consistent with hypothesis idea that different signaling mechanisms are responsible for the specific responses against different bacterial pathogens.

To determine whether expression of any of these ligands is induced in response to pathogen, we used qRT-PCR to evaluate expression levels of genes encoding TGF-β ligands in wild-type animals. Upon 24-hour exposure to *P. luminescens* bacteria, the relative expression of all five TGF-β ligand genes demonstrated no significant alteration compared to control conditions (Fig. 2C). Additionally, analysis of a *dbl-1* transcriptional reporter showed no change in fluorescence

levels on pathogen compared to control bacteria (Fig. S2). We conclude that, although these ligands function in response to pathogen, they are not subject to widespread transcriptional induction.

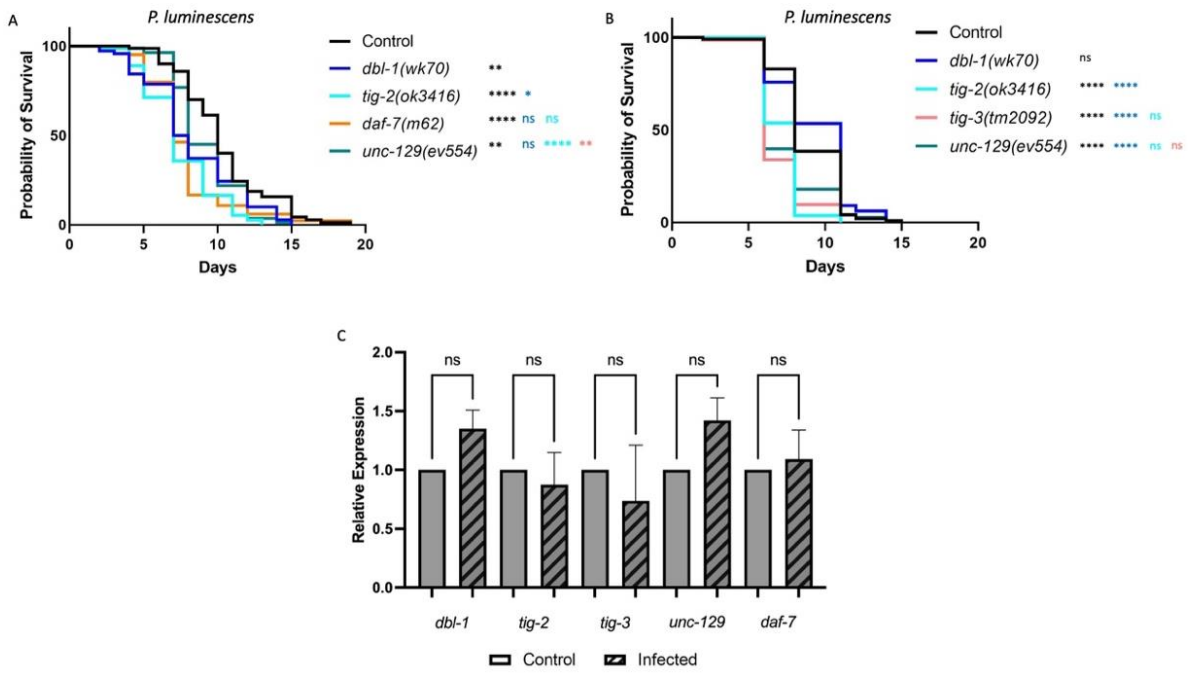


**Figure 2. Five TGF-β Ligands Demonstrate Involvement in Survival Against Bacterial Infection.**

**A**. Survival of TGF-β ligand mutants on *P. luminescens* bacteria. For this trial, strains were grown at 15ºC to avoid dauer formation by *daf-7* mutants and shifted to 20ºC at L4 when exposed to pathogen. n values: Control (70), *dbl-1* (70), *tig-2* (73), *daf-7* (84), *unc-129* (82). **B.** Survival of TGF-β ligand mutants on *P. luminescens* bacteria. n values: Control (99), *dbl-1* (99), *tig-2* (108), *tig-3* (62), *unc-129* (73). **C.** qRT-PCR analysis showing relative expression of TGF-β ligand genes upon 24-hour exposure to *P. luminescens* in Control animals. qRT-PCR data represents repeated analyses of two biological replicates. Statistical analysis done using One-way ANOVA with multiple comparison test. For survivals, statistical analysis done using Log-rank (Mantel-Cox) Test. ns $p > 0.05$; * $p \leq 0.05$; ** $p \leq 0.01$; **** $p < 0.0001$. Black asterisks denote significance relative to control, blue is significance relative to *dbl-1*, teal is significance

relative to *tig-2*, orange is significance relative to *daf-7*, and salmon is significance relative to *tig-3*.

**Multiple TGF-β Ligand Pairs Demonstrate Cooperative Interaction in the *C. elegans* Response to Bacterial Infection**

We next looked for interactions between the remaining *C. elegans* TGF-β ligands upon exposure to bacterial infection by testing double mutants as previously described for *tig-2dbl-1*. We analyzed the *tig-3;tig-2* double mutant, deficient in both the BMP-like ligand TIG-2 and the TGF-β/Activin-like ligand TIG-3, for survival on *P. luminescens*. We found that when grown on bacterial pathogen the *tig-3;tig-2* double mutants demonstrated a survival pattern not significantly different from either the *tig-2* or the *tig-3* single mutants (Fig. 3A). This result contrasts with our analysis of the BMP-like ligands DBL-1 and TIG-2, and suggests that TIG-2/BMP and TIG-3/TGF-β/Activin are acting in the immune response in a cooperative manner.

We also assessed the survival pattern of *daf-7;dbl-1* double mutants on pathogenic bacteria. For this experiment, animals were grown at 15 $^{o}$C to minimize dauer entry in *daf-7* mutants. Survival of *daf-7;dbl-1* double mutants was not significantly different compared to *dbl-1* single mutants (Fig. 3B). The survival pattern of *daf-7;dbl-1* double mutant animals indicates a potential relationship in which both ligands function in a single pathway. This cooperativity is intriguing as the BMP-like ligand DBL-1 is known to signal through a different Type I receptor and different Smads than the TGF-β/Activin-like ligand DAF-7.

Finally, we compared the survival pattern of double and triples mutant for *unc-129*. Although *unc-129* mutants have weak and variable effects on survival, the *unc-129* gene did show some potential interactions with other ligand genes. Survival of *unc-129;tig-2* double mutants are not

significantly different from *tig-2* single mutants (Fig. S1). In contrast, in *tig-3;unc-129* double mutants, the decreased survival of *tig-3* mutants is suppressed (Fig. S2), suggesting a potential antagonistic interaction between UNC-129 and TIG-3. Overall, our results from these survival analyses indicate a complex relationship between the TGF-β family ligands in the immune response. Most surprisingly, ligands that demonstrate cooperative relationships are those from different classes of TGF-β ligands – BMP-like TIG-2 with TGF-β/Activin-like TIG-2; and possibly BMP-like DBL-1 with TGF-β/Activin-like DAF-7.

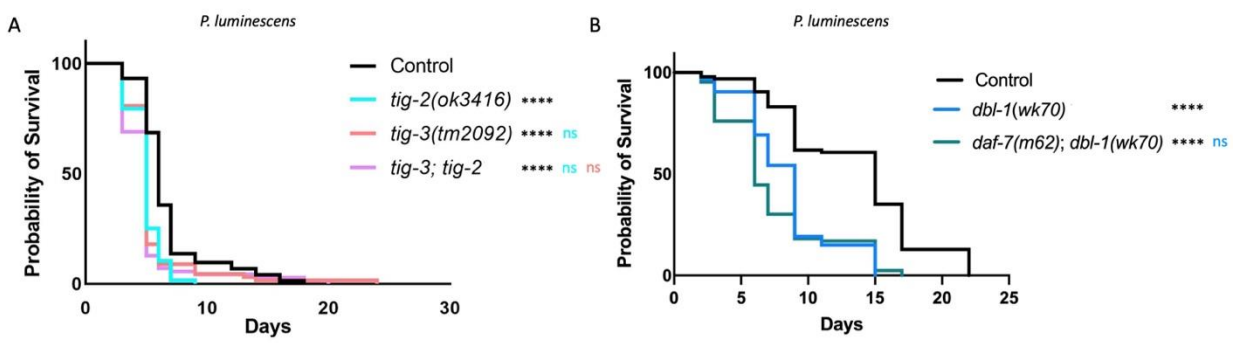


**Figure 3. Multiple TGF-β Ligands Demonstrate Cooperative Interaction in the *C. elegans* Response to Bacterial Infection.**

**A.** Survival analysis of *tig-3(tm2092); tig-2(ok3416)* double mutants on *P. luminescens* bacteria. n values: Control (73), *tig-2* (68), *tig-3* (67), *tig-3;tig-2* (71). **B.** Survival analysis of *daf-7(m62); dbl-1(wk70)* double mutants on *P. luminescens* bacteria. n values: Control (94), *dbl-1* (94), *daf-7* (83). For this trial, strains were grown at 15ºC to avoid dauer formation by *daf-7* mutants and shifted to 20ºC at L4 when exposed to pathogen. Statistical analysis done using Log-rank (Mantel-Cox) Test. ns $p > 0.05$; **** $p < 0.0001$. Black asterisks show significance relative to control, blue is significance relative to *dbl-1*, teal is significance relative to *tig-2*, and salmon is significance relative to *tig-3*.

**Canonical BMP Signaling Components are Involved in the *C. elegans* Immune Response**

The two TGF-β pathways in *C. elegans* are known to signal through canonical mechanisms upon activation. DBL-1 signals through the BMP-like pathway with ligand binding to the single Type II receptor DAF-4 and the Type I receptor SMA-6. The BMP pathway Smads – SMA-2, SMA-3, and SMA-4 – transduce the intracellular signal allowing for gene regulation. The TGF-β/Activin-like ligand DAF-7 signals through the TGF-β/Activin-like pathway components, including the Type I receptor DAF-1 and the Smads DAF-8, DAF-14, and DAF-3 (Estevez *et al.*, 1993; Savage *et al.*, 1996; Suzuki *et al.*, 1999; Krishna *et al.*, 1999; Savage-Dunn and Padgett, 2017). Both pathways converge on the single Type II receptor DAF-4. Previous work has shown that in response to fungal infection of the hypodermis, DBL-1 signals in a pathway utilizing only one receptor-regulated Smad (R-Smad SMA-3) without its typical partner R-Smad SMA-2 or the Co-Smad SMA-4 (Zugasti and Ewbank, 2009). Signaling without a Co-Smad is considered non-canonical. We were therefore interested in which components of the BMP-like and TGF-β/Activin-like pathways are required during bacterial infection and whether non-canonical mechanisms are invoked.

Our survival analysis of DBL-1 pathway components shows a consistently reduced survival pattern for R-Smad mutants *sma-2* and *sma-3* as well as for Co-Smad mutant *sma-4* (Fig. 4A). This result is consistent with a significant role for the BMP pathway Smads in the *C. elegans* response to bacterial pathogen, unlike the results previously shown on fungal infection. Survival analysis of BMP pathway receptors showed a reduced survival pattern for the BMP Type I receptor mutant *sma-6* (Fig. 4B). We observe consistently reduced survival for *sma-6* mutants,

however there is slight variability in the significance of the survival rate for these mutants amongst our trials.

We analyzed the survival patterns of the DAF-7 pathway mutants grown at 15 $^{o}$C on *P. luminescens* bacteria, and found either no phenotype or a mild survival deficit. In particular, R-Smad mutant *daf-8* demonstrated a slightly reduced rate of survival (Fig. 4C), while neither R-Smad mutant *daf-14* (Fig. 4C) nor Type I receptor *daf-1*(Fig. 4D) had significantly altered survival compared to control animals. Thus, although TGF-β/Activin-like ligands DAF-7 and TIG-3 play a role in the immune response against bacterial pathogen, they are unlikely to signal through the canonical TGF-β/Activin signaling components.

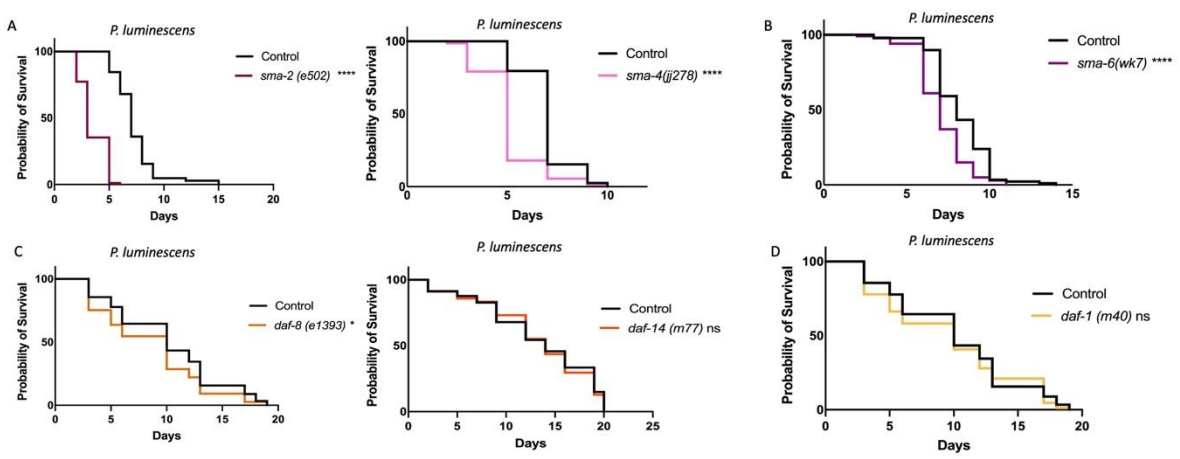


**Figure 4. Canonical BMP Signaling Components are Involved in the *C. elegans* Immune Response**.

**A**. Survival of DBL-1 R-Smad mutant *sma-2(e502)* and Co-Smad mutant *sma-4(jj278)* on *P. luminescens* bacteria. n values: Control (103), *sma-2* (88), Control (78), *sma-4* (72). **B.** Survival analysis of Type I receptor *sma-6(wk7)* on *P. luminescens*. n values: Control (88), *sma-6* (100). **C.** Survival of DAF-7 pathway R-Smad mutants *daf-8(e1393)* and *daf-14(m77)* on *P. luminescens* bacteria. n values: Control (90), *daf-8* (77), Control (81), *daf-14* (78). **D.** Survival analysis of Type I receptor *daf-1(m40)* on *P. luminescens*. n values: Control (90), *daf-1* (86). Statistical analysis done using Log-rank (Mantel-Cox) Test. ns $p > 0.05$; * $p \leq 0.05$; **** $p < 0.0001$.

### *tig-2* and *tig-3* Animals Share Reduced Survival and Pumping Rate Phenotypes with *sma-3* Mutants

Thus far, we have shown that TIG-2/BMP and TIG-3/TGF-β/Activin play more significant roles in survival on *P. luminescens* bacteria than does DBL-1/BMP, and that BMP signaling components play a more significant role than TGF-β/Activin signaling components. These observations suggest a model in which TIG-2 and TIG-3 signal through components previously presumed to respond to DBL-1. To test this model, we compared *tig-2* and *tig-3* phenotypes with those of *sma-3* and *dbl-1*. Survival analysis directly comparing *dbl-1* and *sma-3* mutants on *P. luminescens* demonstrates that while both strains have a decreased survival pattern as compared to control, *sma-3* mutants have a significantly reduced survival rate compared to *dbl-1* mutants (Fig. 5A), suggesting that SMA-3 is responding to other signaling ligands instead of or in addition to DBL-1. Notably, *tig-2* and *tig-3* survival phenotypes are highly similar those of *sma-3* mutants (Fig. 5B), consistent with a model in which TIG-2 and TIG-3 signal through R-Smad SMA-3 in response to *P. luminescens* pathogen.

To test this model further, we analyzed an additional phenotype associated with response to *P. luminescens*, reduced pharyngeal pumping rate (Ciccarelli *et al.*, 2023). We analyzed the pharyngeal pumping rate of these mutants and found that while *dbl-1* mutants do not have a significantly different pumping rate compared to control animals, *sma-3* worms do have a significant reduction in pharyngeal pumping rate and this reduction in pumping is indistinguishable from that of *tig-2* and *tig-3* mutants, as well as the *tig-3;tig-2* double mutant (Fig. 5C-D). This similarity further strengthens the model that TIG-2 and TIG-3 signal through SMA-3 in this context.

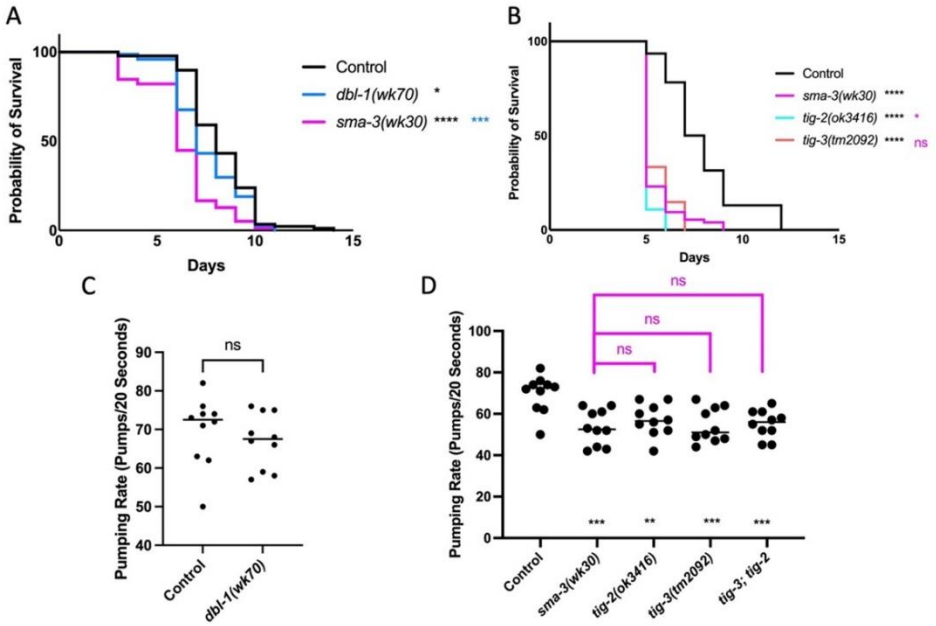


**Figure 5. *tig-2* and *tig-3* Animals Share Reduced Survival and Pumping Rate Phenotypes with *sma-3* Mutants.**

**A.** Survival of *dbl-1(wk70)* and *sma-3(wk30)*. n values: Control (88), *dbl-1* (74), *sma-3* (78). Black asterisks are compared to control. Blue asterisks are compared to *dbl-1*. **B.** Survival of *sma-3(wk30)* mutants compared to *tig-2(ok3416)* and *tig-3(tm2092)*. Black asterisks are compared to control. Pink asterisks are compared to *sma-3*. n values: Control (92), *sma-3* (74), *tig-2* (55), *tig-3* (54). Statistical analysis for all survivals done using Log-rank (Mantel-Cox) test. Survivals were repeated. **C.** Pumping rate per 20 seconds for *dbl-1(wk70)* compared to Control. Statistical analysis done using T-test. **D.** Pumping rate per 20 seconds for *sma-3(wk30), tig-2(ok3416), tig-3(tm2092),* and *tig-3;tig-2*. Black asterisks are compared to Control. Pink asterisks are compared to *sma-3*. Statistical analysis done using One way ANOVA with Multiple Comparison Test. n values for all pumping rate experiments: 10 worms per strain. Pumping rate experiments were repeated on independent biological samples. ns $p > 0.05$; * $p \leq 0.05$; ** $p \leq 0.01$; *** $p \leq 0.001$; **** $p < 0.0001$.

## Structural Modeling of Potential Protein-Protein Interaction Between TIG-2/BMP and TIG-3/TGF-β/Activin

The cooperative action observed between TIG-2/BMP and TIG-3/TGF-β/Activin in the *C. elegans* immune response could be evidence of TIG-2:TIG-3 heterodimers. Alternatively, homodimers of TIG-2 and of TIG-3 could act together through a receptor clustering mechanism (Ramachandran *et al*., 2018). To determine whether heterodimers of TIG-2 and TIG-3 are feasible, we performed structural modeling *in silico.* Using the ColabFold (Mirdita *et al*., 2022) implementation of AlphaFold (Jumper *et al*., 2021), we asked whether confident structural predictions could be made for TIG-2 homodimers, TIG-3 homodimers, and TIG-2:TIG-3 heterodimers. Using the mature bioactive domain of TIG-2, we were able to generate a strongly supported model for the TIG-2 homodimer that recapitulates the well-known "butterfly" structure of TGF-β family ligand dimers (Fig. 6). In contrast, the potential for the TIG-3 mature bioactive domain to form homodimers was not well supported by ColabFold, with a poor interface predicted template modeling (ipTM) score of 0.246. Using TIG-2 and TIG-3 for modeling, however, resulted in a heterodimer with a high ipTM score of 0.803, similar to that of the TIG-2 homodimer (0.87). Furthermore, in the TIG-2 homodimer and TIG-2:TIG-3 heterodimer predictions, cysteine residues are well placed for the formation of interchain disulfide bonds (yellow rods in Fig. 6). In contrast, in models of TIG-3 homomeric interaction, no cysteine residues are present at the interface to form disulfide bonds, and the equivalent cysteine residues are well separated (highlighted in yellow within a β strand in the model). In vivo, prodomains present in the uncleaved precursors have been shown to be required for heterodimer formation between BMP4 and BMP7 (Neugebauer *et al.*, 2015). We therefore performed structural modeling with full-length proteins (prodomain + mature domain), and

similar results were obtained. For TIG-2 and TIG-3 to form heterodimers in vivo, they must be expressed in the same cell type. In fact, their expression does overlap in neurons such as AFD and M2. These neurons are located adjacent to the pharynx. We have shown that SMA-3/Smad is required in pharyngeal muscle for survival on bacterial pathogens (Ciccarelli *et al.,* 2023), so TIG-2 and TIG-3 are produced in a location appropriate for signaling to SMA-3/Smad in the pharynx. Therefore, *in silico* modeling and overlapping expression patterns support the possibility of a TIG-2:TIG-3 heterodimer that would be consistent with our functional genetic analysis. This model can now be tested with biochemical analysis of protein-protein interactions.

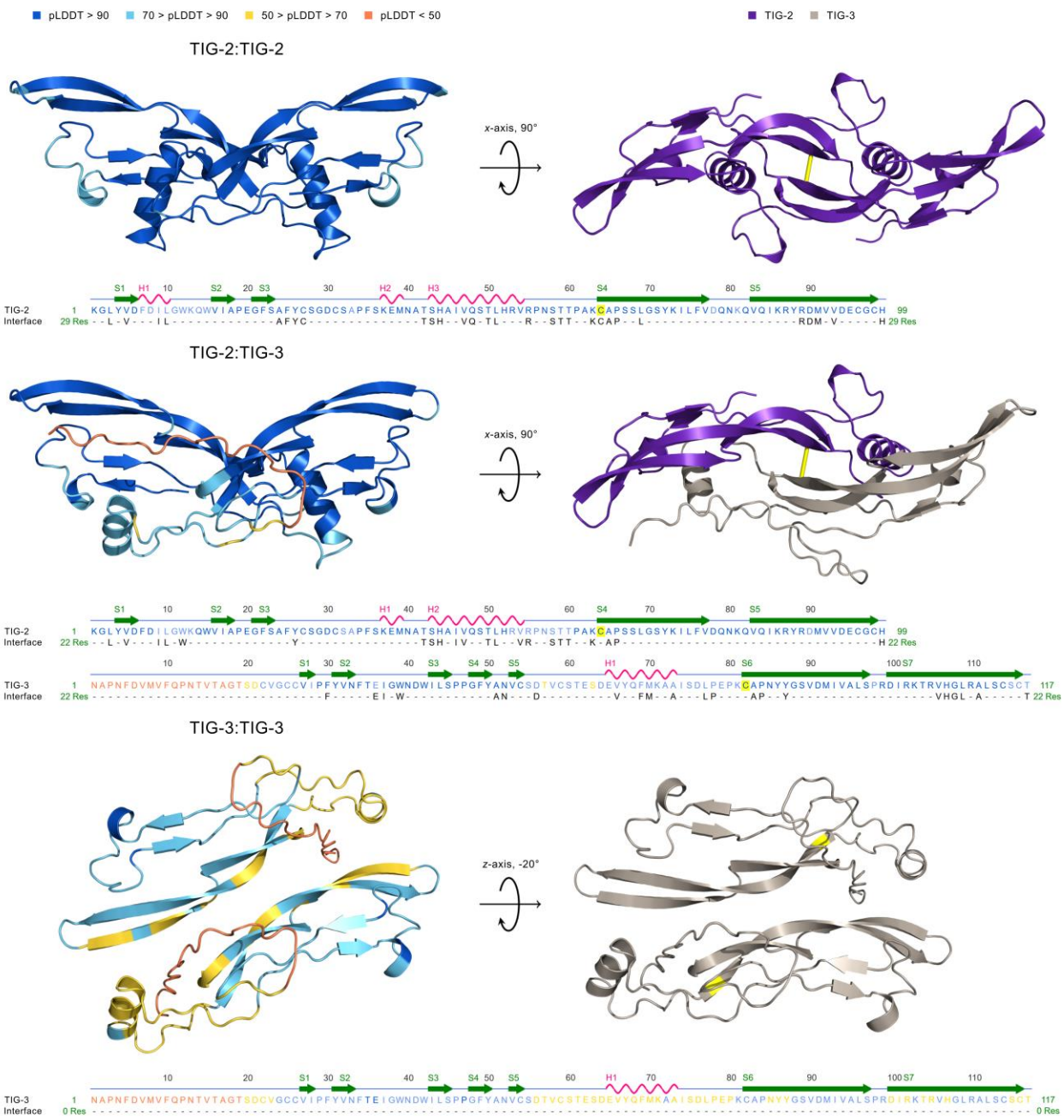


**Figure 6. Structural Modeling of TIG-2 and TIG-3 Mature Ligand Homo- and Hetero-dimer Complexes Using AlphaFold2.** Left complex: 3D structures are colored by pLDDT confidence score with deep blue corresponding to regions of very high confidence and orange representing regions of very low confidence or disorder. Right complex: The dimer (TIG-2 in purple, TIG-3 in beige) following geometric rotation to emphasize either a potential interchain

disulfide interaction or the noninteracting Cys82 residues in TIG-3:TIG-3. 1D Sequence: Residues are colored by pLDDT with cysteines of interest highlighted in yellow. Secondary structure annotation and indexing are displayed in the top row. The bottom row "Interface" track consists of confidently predicted (see Methods) dimer-interface contacts within a distance of 4 Å. TIG-2:TIG-2 exhibits high confidence with respect to structural modeling and dimeric interaction (pLDDT: 93.8, pTM: 0.855, ipTM: 0.87), and contains a candidate interchain (64-64) disulfide species. TIG-2:TIG-3 is confidently modeled regarding its structure and capacity for dimerization (pLDDT: 85.9, pTM: 0.793, ipTM: 0.803), and possesses a potential interchain (64-82) disulfide species. The quality of the structural prediction for TIG-3:TIG-3 (pLDDT: 66.6) is slightly below the threshold of acceptable confidence (pLDDT > 70) and its predicted ability to homodimerize is very low (ipTM: 0.246). Additionally, no confidently-predicted (pTM: 0.498) interface residues exist or interchain cysteine pairs within 8 Å.

## Discussion

The multiplicity of TGF-β family ligands, receptors, and Smad signal transducers may support the generation of diverse context-dependent outcomes through combinatorial interactions. Biochemical and computational approaches are powerful to identify the principles mediating the potential protein-protein interactions between these components, but these approaches must be complemented by functional in vivo analyses. The nematode *C. elegans* has five TGF-β ligands and two characterized TGF-β family signaling pathways (Patterson and Padgett, 2000; MacNeill *et al.*, 2009), providing a powerful in vivo system in which to study TGF-β ligand functions in the context of the intact organism. Critically, TGF-β signaling mechanisms are conserved in this organism. Here we demonstrate that all five TGF-β ligands play a role in the immune response against bacterial pathogen. Furthermore, two ligand pairs consisting of a BMP subfamily and a TGF-β/Activin subfamily member (TIG-2/TIG-3 and DBL-1/DAF-7) show evidence of acting together in the response to gram-negative bacterium *P. luminescens.*

These studies were initiated with the well characterized BMP-like DBL-1 signaling pathway, which is associated with significant roles in development and body size regulation but has also been shown to play an important role in the immune response against both bacterial and fungal pathogens (Mallo, 2002; Tenor and Aballay, 2008; Zugasti and Ewbank, 2009). Comparing the response to the gram-negative bacteria *S. marcescens* and *P. luminescens*, we obtained evidence implicating a level of specificity of ligand responses for particular bacteria. Although both BMP-like ligands, DBL-1 and TIG-2, play a significant role in the response against *S. marcescens*, TIG-2 has a more significant role than DBL-1 in the response against *P. luminescens*. These results suggest that the function of DBL-1 in the immune response is not a general one-size-fits-

all response to bacterial pathogen but rather a more nuanced response with some level of pathogen specificity. Furthermore, we show that DBL-1/BMP and TIG-2/BMP have additive roles in the response to *P. luminescens,* suggesting that they trigger independent responses. The orphan ligand UNC-129 shows moderate and variably significant changes in survival on *P. luminescens,* suggesting a minor or modulatory role. The TGF-β/Activin-like ligands DAF-7 and TIG-3 demonstrated consistently significant reduced survival patterns on *P. luminescens* suggesting involvement of these ligands in the response to this bacterial pathogen. qRT-PCR analysis of TGF-β ligand expression shows that with 24-hour exposure to bacterial infection, expression levels of the ligands do not significantly change from control conditions. A *dbl-1p*::GFP transcriptional reporter validates these results for *dbl-1*. Taken together, we conclude that all five of the TGF-β ligands play a role in the immune response, but not at the level of transcriptional induction.

Analysis of the survival patterns of double mutant animals produced results indicating interactions between multiple TGF-β family ligands. Interestingly, the interactions between pairs of BMP-like and TGF-β/Activin-like ligands suggest cooperative interaction in a common pathway. Specifically, the *tig-3; tig-2* double mutant survival pattern is no more severe than either single mutant alone. Similarly, the *daf-7; dbl-1* double mutant survival is indistinguishable from that of *dbl-1* single mutants. Of these pairs, TIG-2 and TIG-3 play a more major role in the response to *P. luminescens.* We therefore used computational modeling to determine whether these ligands could feasibly function as a heterodimer. Using ColabFold, we demonstrated that a TIG-2:TIG-3 heterodimer is better supported than the TIG-3 homodimer. Furthermore, given that these ligands have overlapping expression patterns, it is possible that they form heterodimers in vivo. We also identify the canonical BMP-like pathway as required for response to *P.*

*luminescens*, including the Type I receptor (SMA-6), the R-Smads (SMA-2 and SMA-3) and Co-Smad (SMA-4). In contrast, TGF-β/Activin pathway components have minimal effects. Unlike *dbl-1* mutants, *tig-2* and *tig-3* mutants have very similar survival phenotypes to *sma-3* mutants. Furthermore, *tig-2, tig-3,* and *sma-3* mutants share a pharyngeal pumping defect that is not seen in *dbl-1* mutants. These similarities provide evidence that TIG-2 and TIG-3 signal through the canonical BMP signaling pathway consisting of SMA-6 Type I receptor, and SMA-2, SMA-3, and SMA-4 Smads in the context of bacterial pathogen survival. There is precedence for TGF-β/Activin ligands signaling through BMP-like signaling pathways in vertebrates. For example, in endothelial cells, TGF-β can phosphorylate presumptive BMP Smads Smad1/5 through interaction with type I receptor ALK1 rather than ALK5 (Lebrin *et al.,* 2005). Furthermore, the BMP receptor ALK2 (ACVR1) can be activated by Activin to phosphorylate Smad1/5, and this activity is increased by pathogenic FOP mutations (Ramachandran *et al.,* 2021). However, cooperative action between a BMP and TGF-β/Activin ligand, including potential cross-family heterodimers, has not yet been described in vertebrates to our knowledge, and warrants further consideration.

Interestingly, nonredundant roles for TIG-2, TIG-3, and UNC-129 have recently been identified in neuronal guidance in *C. elegans* (Baltaci *et al.,* 2022). In neuronal guidance, TIG-3:UNC-129 heterodimers are implicated, with TIG-2 being released from a different tissue. In this context, the ligands depend on the BMP signaling components SMA-6 Type I Receptor and SMA-2, SMA-3, and SMA-4 Smads. Relatedly, in Drosophila, three Activin ligands are required nonredundantly to regulate photoreceptor identity through the canonical Activin signaling components (Wells *et al.,* 2017). In addition to heterodimers, nonredundant functions of TGF-β

ligands can be explained by a receptor clustering mechanism that generates higher-order signaling complexes (Ramachandran *et al.*, 2018). Our system provides a platform for studying the functional interactions between multiple TGF-β ligands. Cooperativity between BMP and TGF-β/Activin subfamily members may provide a mechanism for distinguishing the developmental and homeostatic functions of these ligands from an acute response such as the innate immune response to bacterial pathogens.

**Acknowledgements**

This work was funded by R15GM112147 to CSD (National Institutes of Health/NIGMS). Some strains were provided by the Caenorhabditis Genetics Center, which is supported by the National Institute of Health - Office of Research Infrastructure Programs (P40 OD010440). We are grateful to the lab of Roger Pocock for sharing double and triple mutants of TGF-β ligand genes. We thank Jan Christian for helpful comments on the manuscript. This work was carried out in partial fulfillment of the requirements for the Ph.D. degree from the Graduate Center of City University of New York (EJC).

## References


Attisano L, Wrana JL. 1996. Signal transduction by members of the transforming growth factor-beta superfamily. *Cytokine Growth Factor Rev* **7**:327–339. doi:(Kim et al., 2019)

Aykul S, Martinez-Hackert E. 2016. Transforming Growth Factor-β Family Ligands Can Function as Antagonists by Competing for Type II Receptor Binding. *J Biol Chem* **291**:10792–10804. doi:10.1074/jbc.M115.713487

Baltaci O, Pedersen ME, Sherry T, Handley A, Snieckute G, Cao W, Haas M, Archer S, Pocock R. 2022. Atypical TGF-β signaling controls neuronal guidance in Caenorhabditis elegans. *iScience* **25**:103791. doi:10.1016/j.isci.2022.103791

Blobe GC, Schiemann WP, Lodish HF. 2000. Role of transforming growth factor beta in human disease. *N Engl J Med* **342**:1350–1358. doi:10.1056/NEJM200005043421807

Ciccarelli EJ, Bendelstein M, Savage-Dunn C. 2023. BMP signaling to pharyngeal muscle in the *C. elegans* immune response to bacterial pathogen regulates anti-microbial peptide expression and pharyngeal pumping. doi: 10.1101/2023.03.06.531324

Derynck R, Akhurst RJ, Balmain A. 2001. TGF-beta signaling in tumor suppression and cancer progression. *Nat Genet* **29**:117–129. doi:10.1038/ng1001-117

Derynck R, Zhang Y, Feng XH. 1998. Smads: transcriptional activators of TGF-beta responses. *Cell* **95**:737–740. doi:10.1016/s0092-8674(00)81696-7

Estevez M, Attisano L, Wrana JL, Albert PS, Massagué J, Riddle DL. 1993. The daf-4 gene encodes a bone morphogenetic protein receptor controlling C. elegans dauer larva development. *Nature* **365**:644–649. doi:10.1038/365644a0

Georgi LL, Albert PS, Riddle DL. 1990. daf-1, a C. elegans gene controlling dauer larva development, encodes a novel receptor protein kinase. *Cell* **61**:635–645. doi:10.1016/0092-8674(90)90475-t

Herpin A, Lelong C, Favrel P. 2004. Transforming growth factor-beta-related proteins: an ancestral and widespread superfamily of cytokines in metazoans. *Dev Comp Immunol* **28**:461–485. doi:10.1016/j.dci.2003.09.007

Hoffmann JA, Kafatos FC, Janeway CA, Ezekowitz RA. 1999. Phylogenetic perspectives in innate immunity. *Science* **284**:1313–1318. doi:10.1126/science.284.5418.1313

Huminiecki L, Goldovsky L, Freilich S, Moustakas A, Ouzounis C, Heldin C-H. 2009. Emergence, development and diversification of the TGF-βsignalling pathway within the animal kingdom. *BMC Evolutionary Biology* **9**:28. doi:10.1186/1471-2148-9-28

Irazoqui JE, Ng A, Xavier RJ, Ausubel FM. 2008. Role for beta-catenin and HOX transcription factors in Caenorhabditis elegans and mammalian host epithelial-pathogen interactions. *Proc Natl Acad Sci U S A* **105**:17469–17474. doi:10.1073/pnas.0809527105

Jumper J, Evans R, Pritzel A, Green T, Figurnov M, Ronneberger O, Tunyasuvunakool K, Bates R, Žídek A, Potapenko A, Bridgland A, Meyer C, Kohl SAA, Ballard AJ, Cowie A, Romera-Paredes B, Nikolov S, Jain R, Adler J, Back T, Petersen S, Reiman D, Clancy E, Zielinski M, Steinegger M, Pacholska M, Berghammer T, Bodenstein S, Silver D, Vinyals O, Senior AW, Kavukcuoglu K, Kohli P, Hassabis D. 2021. Highly accurate protein structure prediction with AlphaFold. *Nature* **596**:583–589. doi:10.1038/s41586-021-03819-2

Kim DH, Feinbaum R, Alloing G, Emerson FE, Garsin DA, Inoue H, Tanaka-Hino M, Hisamoto N, Matsumoto K, Tan M-W, Ausubel FM. 2002. A conserved p38 MAP kinase pathway in Caenorhabditis elegans innate immunity. *Science* **297**:623–626. doi:10.1126/science.1073759

Kim H-S, Neugebauer J, McKnite A, Tilak A, Christian JL. 2019. BMP7 functions predominantly as a heterodimer with BMP2 or BMP4 during mammalian embryogenesis. *eLife* **8**:e48872. doi:10.7554/eLife.48872

Krishna S, Maduzia LL, Padgett RW. 1999. Specificity of TGFbeta signaling is conferred by distinct type I receptors and their associated SMAD proteins in Caenorhabditis elegans. *Development* **126**:251–260. doi:10.1242/dev.126.2.251

Lebrin F, Deckers M, Bertolino P, Ten Dijke P. 2005. TGF-beta receptor function in the edothelium. Cardiovasc Res **65**:599-608. doi: 10.1016/j.cardiores.2004.10.036.

Li M, Wan Y, Sanjabi S, Robertson A-K, Flavell R. 2006. Transforming growth factor-regulation of immune responses. *Annual Review of Immunology* **24:**99-146. doi: 10.1146/annurev.immunol.24.021605.090737

Little SC, Mullins MC. 2009. Bone morphogenetic protein heterodimers assemble heteromeric type I receptor complexes to pattern the dorsoventral axis. *Nat Cell Biol* **11**:637–643. doi:10.1038/ncb1870

MacNeil LT, Hardy WR, Pawson T, Wrana JL, Culotti JG. 2009. UNC-129 regulates the balance between UNC-40 dependent and independent UNC-5 signaling pathways. *Nat Neurosci* **12**:150–155. doi:10.1038/nn.2256

Mallo GV, Kurz CL, Couillault C, Pujol N, Granjeaud S, Kohara Y, Ewbank JJ. 2002. Inducible antibacterial defense system in C. elegans. *Curr Biol* **12**:1209–1214. doi:10.1016/s0960-9822(02)00928-4

Massagué J. 2012. TGFβ signalling in context. *Nat Rev Mol Cell Biol* **13**:616–630. doi:10.1038/nrm3434

Massagué J. 2008. TGFbeta in Cancer. *Cell* **134**:215–230. doi:10.1016/j.cell.2008.07.001

Massagué J. 1998. TGF-beta signal transduction. *Annu Rev Biochem* **67**:753–791. doi:10.1146/annurev.biochem.67.1.753

Massagué J, Chen YG. 2000. Controlling TGF-beta signaling. *Genes Dev* **14**:627–644.

Medzhitov R, Janeway CA. 1998. Innate immune recognition and control of adaptive immune responses. *Semin Immunol* **10**:351–353. doi:10.1006/smim.1998.0136

Millet ACM, Ewbank JJ. 2004. Immunity in Caenorhabditis elegans. *Curr Opin Immunol* **16**:4–9. doi:10.1016/j.coi.2003.11.005

Mirdita M, Schütze K, Moriwaki Y, Heo L, Ovchinnikov S, Steinegger M. 2022. ColabFold: making protein folding accessible to all. *Nat Methods* **19**:679–682. doi:10.1038/s41592-022-01488-1

Morita K, Flemming AJ, Sugihara Y, Mochii M, Suzuki Y, Yoshida S, Wood WB, Kohara Y, Leroi AM, Ueno N. 2002. A Caenorhabditis elegans TGF-β, DBL-1, controls the expression of LON-1, a PR-related protein, that regulates polyploidization and body length. *EMBO J* **21**:1063–1073. doi:10.1093/emboj/21.5.1063

Neugebauer JM, Kwon S, Kim HS, Donley N, Tilak A, Sopory S, Christian JL. 2015. The prodomain of BMP4 is necessary and sufficient to generate stable BMP4/7 heterodimers with enhanced bioactivity in vivo. *Proc Natl Acad Sci USA* **112**:E2307-16. doi: 10.1073/pnas.1501449112.

Partridge FA, Gravato-Nobre MJ, Hodgkin J. 2010. Signal transduction pathways that function in both development and innate immunity. *Developmental Dynamics* **239**:1330–1336. doi:10.1002/dvdy.22232

Patterson GI, Padgett RW. 2000. TGF beta-related pathways. Roles in Caenorhabditis elegans development. *Trends Genet* **16**:27–33. doi:10.1016/s0168-9525(99)01916-2

Pohlers D, Brenmoehl J, Löffler I, Müller CK, Leipner C, Schultze-Mosgau S, Stallmach A, Kinne RW, Wolf G. 2009. TGF-beta and fibrosis in different organs - molecular pathway imprints. *Biochim Biophys Acta* **1792**:746–756. doi:10.1016/j.bbadis.2009.06.004

Principe DR, Doll JA, Bauer J, Jung B, Munshi HG, Bartholin L, Pasche B, Lee C, Grippo PJ. 2014. TGF-β: duality of function between tumor prevention and carcinogenesis. *J Natl Cancer Inst* **106**:djt369. doi:10.1093/jnci/djt369

Ramachandran A, Vizán P, Das D, Chakravarty P, Vogt J, Rogers KW, Müller P, Hinck AP, Sapkota GP, Hill CS. 2018. TGF-β uses a novel mode of receptor activation to phosphorylate SMAD1/5 and induce epithelial-to-mesenchymal transition. *eLife* **7**:e31756. doi:10.7554/eLife.31756

Ramachandran A, Mehić M, Wasim L, Malinova D, Gori I, Blaszczyk BK, Carvalho DM, Shore EM, Jones C, Hyvönen M, Tolar P, Hill CS. 2021. Pathogenic ACVR1$^{R206H}$ activation by

activin A-induced receptor clustering and autophosphorylation. *EMBO J* **40**:e106317. doi: 10.15252/embj.2020106317

Savage C, Das P, Finelli AL, Townsend SR, Sun CY, Baird SE, Padgett RW. 1996. Caenorhabditis elegans genes sma-2, sma-3, and sma-4 define a conserved family of transforming growth factor beta pathway components. *Proc Natl Acad Sci U S A* **93**:790–794. doi:10.1073/pnas.93.2.790

Savage-Dunn C, Padgett RW. 2017. The TGF-β Family in Caenorhabditis elegans. *Cold Spring Harb Perspect Biol* **9**:a022178. doi:10.1101/cshperspect.a022178

Schulenburg H, Kurz CL, Ewbank JJ. 2004. Evolution of the innate immune system: the worm perspective. *Immunol Rev* **198**:36–58. doi:10.1111/j.0105-2896.2004.0125.x

Shimmi O, Umulis D, Othmer H, O'Connor MB. 2005. Facilitated transport of a Dpp/Scw heterodimer by Sog/Tsg leads to robust patterning of the Drosophila blastoderm embryo. *Cell* **120**:873–886. doi:10.1016/j.cell.2005.02.009

Silberstein GB, Daniel CW. 1987. Reversible inhibition of mammary gland growth by transforming growth factor-beta. *Science* **237**:291–293. doi:10.1126/science.3474783

Suzuki Y, Yandell MD, Roy PJ, Krishna S, Savage-Dunn C, Ross RM, Padgett RW, Wood WB. 1999. A BMP homolog acts as a dose-dependent regulator of body size and male tail patterning in Caenorhabditis elegans. *Development* **126**:241–250. doi:10.1242/dev.126.2.241

Tenor JL, Aballay A. 2008. A conserved Toll-like receptor is required for Caenorhabditis elegans innate immunity. *EMBO Rep* **9**:103–109. doi:10.1038/sj.embor.7401104

Tillet E, Ouarné M, Desroches-Castan A, Mallet C, Subileau M, Didier R, Lioutsko A, Belthier G, Feige J-J, Bailly S. 2018. A heterodimer formed by bone morphogenetic protein 9 (BMP9) and BMP10 provides most BMP biological activity in plasma. *J Biol Chem* **293**:10963–10974. doi:10.1074/jbc.RA118.002968

Wang J, Tokarz R, Savage-Dunn C. 2002. The expression of TGFbeta signal transducers in the hypodermis regulates body size in C. elegans. *Development* **129**:4989–4998. doi:10.1242/dev.129.21.4989

Wells BS, Pistillo D, Barnhart E, Desplan C. 2017. Parallel Activin and BMP signaling coordinates R7/R8 photoreceptor subtype pairing in the stochastic Drosophila retina. *eLife* **6**:e25301. doi:10.7554/eLife.25301

Wisotzkey RG, Newfeld SJ. 2020. TGF-β prodomain alignments reveal unexpected cysteine conservation consistent with phylogenetic predictions of cross-subfamily heterodimerization. *Genetics* **214**:447-465. doi: 10.1534/genetics.119.302255

Wrana JL. 2013. Signaling by the TGF-β Superfamily. *Cold Spring Harb Perspect Biol* **5**:a011197. doi:10.1101/cshperspect.a011197

Wrana JL, Attisano L, Wieser R, Ventura F, Massagué J. 1994. Mechanism of activation of the TGF-β receptor. *Nature* **370**:341–347. doi:10.1038/370341a0

Yin J, Madaan U, Park A, Aftab N, Savage-Dunn C. 2015. Multiple cis elements and GATA factors regulate a cuticle collagen gene in *Caenorhabditis elegans*. *Genesis* **53**:278-284. doi: 10.1002/dvg.22847

Yoshida S, Morita K, Mochii M, Ueno N. 2001. Hypodermal expression of Caenorhabditis elegans TGF-beta type I receptor SMA-6 is essential for the growth and maintenance of body length. *Dev Biol* **240**:32–45. doi:10.1006/dbio.2001.0443

Zamarron BF, Chen W. 2011. Dual roles of immune cells and their factors in cancer development and progression. *Int J Biol Sci* **7**:651–658. doi:10.7150/ijbs.7.651

**Supplemental Figures**

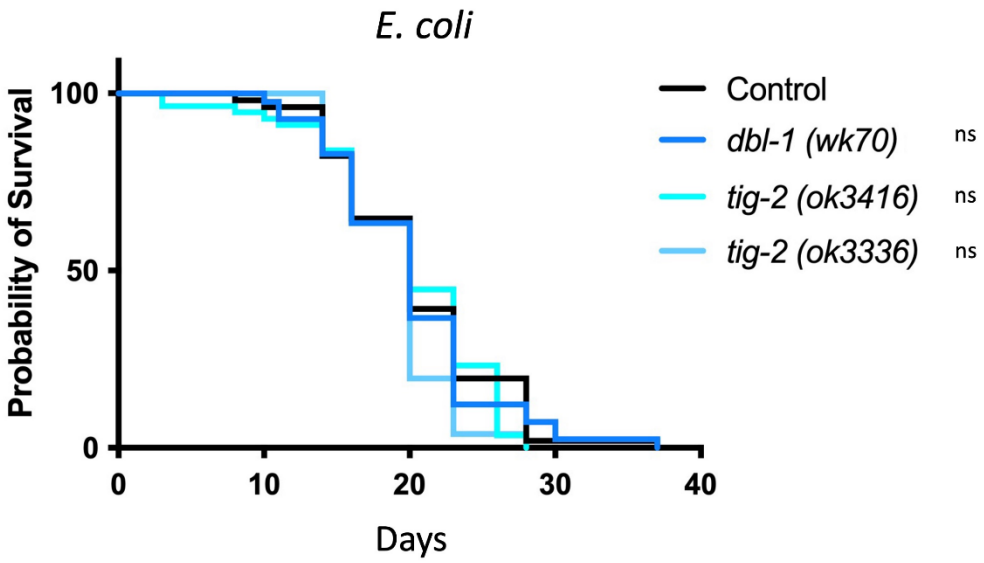


Figure S1. Lifespan analysis of *dbl-1(wk70)*, *tig-2(ok3416)*, and *tig-2(ok3336)* on nonpathogenic *E. coli* strain DA837. n values: Control (51), *dbl-1* (41), *tig-2* (56), *tig-2* (51).

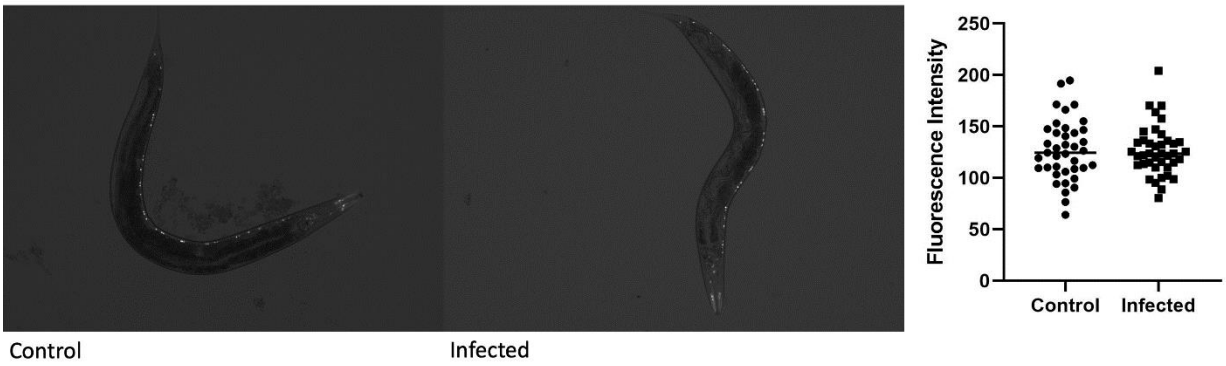


Figure S2. Reporter imaging of *dbl-1p::*GFP transcriptional reporter on control *E.* coli and 24-hour infection on *P. luminescens* bacteria. No significance.

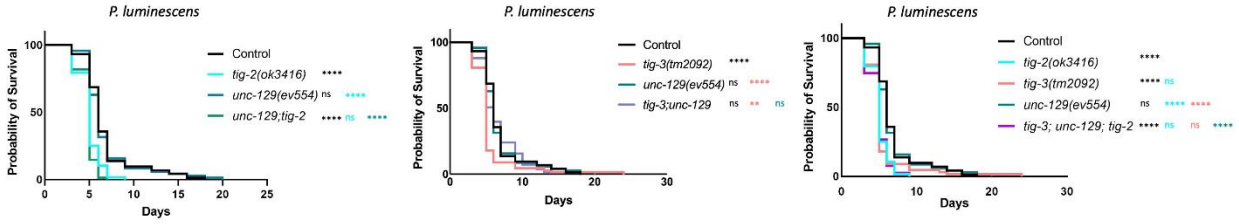


Figure S3. Survival analysis of *unc-129(ev554);tig-2(3416), unc-129(ev554);tig-3(tm2092),* and *tig-3(tm2092);unc-129(ev554);tig-2(ok3416)*. n values: Control (73), *tig-2* (68), *unc-129* (70), *unc-129;tig-2* (83), *tig-3* (67), *tig-3;unc-129* (83), *tig-3;unc-129;tig-2* (79). Statistical analysis for survival analyses done using Log-rank (Mantel-Cox) Test.